Field calibration of sediment flux dependent river incision

Field calibration of sediment flux dependent river incision

Daniel E. J. Hobley,[1,2] Hugh D. Sinclair,[1] Simon M. Mudd,[1,3] and Patience A. Cowie[4]

[1] Bed erosion and sediment transport are ubiquitous and linked processes in rivers. Erosion can either be modeled as a "detachment limited" function of the shear stress exerted by the flow on the bed, or as a "transport limited" function of the sediment flux capacity of the flow. These two models predict similar channel profiles when erosion rates are constant in space in time, but starkly contrasting behavior in transient settings. Traditionally detachment limited models have been used for bedrock rivers, whereas transport limited models have been used in alluvial settings. In this study we demonstrate that rivers incising into a substrate of loose, but very poorly sorted relict glacial sediment behave in a detachment limited manner. We then develop a methodology by which to both test the appropriate incision model and constrain its form. Specifically we are able to tightly constrain how incision rates vary as a function of the ratio between sediment flux and sediment transport capacity in three rivers responding to deglaciation in the Ladakh Himalaya, northwest India. This represents the first field test of the so-called "tools and cover" effect along individual rivers.

1. Introduction

[2] River dynamics in upland settings are a key element in the Earth surface system, redistributing large volumes of sediment into basins [*Milliman and Syvitski*, 1992], coupling climate and tectonic processes [*Molnar and England*, 1990; *Willett and Brandon*, 2002], transmitting information from downstream into highlands [*Rodríguez-Iturbe et al.*, 1992], and controlling the form of mountain belts themselves [*Burbank*, 2002; *Zeitler et al.*, 2001]. However, significant uncertainty still remains over how real river systems are likely to evolve through time. Numerous models of river erosion have been proposed [see, e.g., *Tucker and Hancock*, 2010], but much doubt remains over how we should distinguish between these models and whether factors such as thresholds and sediment flux dependent incision are important in real settings. This is vital to establish, since the long term tempo, style and patterns of landscape evolution under each modeling approach can be very different [e.g., *Whipple and Tucker*, 2002].

[3] In all incising channels, sediment flux is likely to be of key importance in controlling erosion processes. Where the bed of a channel is entirely composed of loose, readily transportable particles, the divergence of sediment flux capacity of the flow above determines the rate of bed elevation change, as described by a mass balance (i.e., the Exner equation) [e.g., *Paola and Voller*, 2005]. In bedrock channels, where the channel bed resists detachment into the flow, authors have also drawn attention to sediment flux dependent incision. Here, sediment is likely to create a strongly nonlinear erosional response, as it may both promote incision by acting as tools and inhibit it by covering the bed [*Cowie et al.*, 2008; *Gilbert*, 1877; *Sklar and Dietrich*, 2001; *Turowski et al.*, 2007]. However, it has proven difficult to unequivocally demonstrate the form of this effect in real environments, and in particular to prove the existence of positive feedbacks between sediment flux and incision rates.

[4] We set out both to discriminate between incision models and also to assess the role of sediment flux in catchments in Ladakh, northwest Indian Himalaya, the upper reaches of which have been significantly resculpted by glacial processes [*Hobley et al.*, 2010]. This location is ideal for such a study as we may tightly constrain through time both total incision at a point and sediment fluxes downstream as the channels respond. The incised substrate in these valleys is very poorly sorted, thick, relict glacial sediment, with subangular clasts and grain sizes ranging from silts through to meter-scale boulders (Figure 1). It might be expected that since the substrate is composed of individual clasts, many of which are ostensibly ready for transport, its erosion would be controlled by the carrying capacity of the stream. Set against this, field observations suggest that the coarse, angular, poorly sorted texture of the glacial sediment can lead to a partly locked texture of cobble grade and coarser clasts on the bed once part of the fine fraction has been winnowed away, and qualitative interpretation of the beds of the modern streams suggest that the coarser (boulder) fraction in the substrate may play a disproportionate role in

---

[1]School of GeoSciences, University of Edinburgh, Edinburgh, UK.
[2]Department of Environmental Sciences, University of Virginia, Charlottesville, Virginia, USA.
[3]Earth Research Institute, University of California, Santa Barbara, California, USA.
[4]Department of Earth Science, University of Bergen, Bergen, Norway.

Figure 1. Typical view of an incising trunk channel in the Ladakh catchments. The very poorly sorted substrate of glacial sediment is visible in the sidewall on the left bank. The channel itself contains numerous large boulders but is dominated by imbricated, subangular cobbles.

limiting channel downcutting [*Hobley et al.*, 2010]. Such a system could be argued to be more akin to a bedrock channel undergoing erosion by plucking than a true alluvial river. This kind of behavior may be widespread in upland environments where channels are loaded directly by unsorted non-fluvial sediment, for example, in bedrock landslides or debris flows.

[5] The key point is that in this type of setting the basic distinction of erosion style as either transport limited (erosion controlled by carrying capacity) or detachment limited (erosion controlled by shear stress on the bed) is unclear from qualitative field observations. Hence, before we can analyze the role of sediment flux in modulating incision rates, we must choose between these two mutually exclusive options for building the incision law. Firstly, we present an analysis of the detachment and transport limited frameworks for fluvial erosion. We use the downstream distribution of shear stress to demonstrate that, despite the clastic nature of the substrate, the channels in this study are responding in a sediment flux dependent, detachment limited manner above an incision threshold. We are able to rule out a transport limited interpretation. Secondly, we use field observations to constrain the resulting sediment flux functions for each analyzed catchment using a Monte Carlo Markov Chain model. The resulting curves show the operation of both positive and negative feedbacks on erosion rate with varying sediment flux and allow investigation of the factors controlling their expression.

2. Modeling Framework

[6] The long term evolution of fluvial systems has often been described as either detachment limited (DL), governed by resistance of the bed to erosion, or transport limited (TL), governed by capacity of the flow to carry away material which is freely available on the bed [*Anderson*, 1994; *Beaumont et al.*, 1992; *Howard*, 1994; *Kooi and Beaumont*, 1994; *Tucker and Bras*, 1998; *Whipple and Tucker*, 1999,

2002; *Willgoose et al.*, 1991]. These mutually exclusive descriptions of incision are advantageous as they allow modeling of channels in mountain belts across geologically relevant timescales ($>10^4$ years), and represent relatively simple approaches which allow us to approximate the first order kinematics of such systems through time. They do not require a full description of the hydrology of the catchment or the hydraulics of the sediment mobilization processes, which may not be available on long timescales. Both have been shown to produce realistic results when compared to real landscapes [*Attal et al.*, 2008, 2011; *Cowie et al.*, 2006; *Kooi and Beaumont*, 1994; *Loget et al.*, 2006; *Snyder et al.*, 2000; *Stock and Montgomery*, 1999; *Valla et al.*, 2010; *van der Beek and Bishop*, 2003; *Whittaker et al.*, 2008].

2.1. Detachment Limited and Transport Limited River Incision

[7] Many different formulations of the detachment limited approach exist in the literature; the most general of these has been outlined by *Whipple* [2004], as

$$E = k_r k_c k_{\tau c} f(q_s, q_c) A^m S^n \qquad (1)$$

where E is bed erosion rate, k_r, k_c and $k_{\tau c}$ are parameters reflecting bed erodibility, erosivity of the climate, and threshold of incision, respectively, $f(q_s, q_c)$ is a parameter reflecting the influence of sediment load which we shall term the sediment flux function, A and S are the upstream drainage area and local channel slope, and m and n are dimensionless parameters reflecting incision process in the channel, basin hydrology and channel hydraulic geometry. This equation can also be stated explicitly in terms of mean bed shear stress, τ, giving

$$E = K f(q_s, q_c)(\tau - \tau_c)^a \qquad (2)$$

where a is thought to reflect the dominant incision process [*Whipple et al.*, 2000], τ_c is a threshold below which no incision occurs, and K is a parameter reflecting the combined influences of bed erodibility, climatic influence and erosion process [*Hancock et al.*, 1998; *Howard and Kerby*, 1983]. Note that K is not necessarily a constant, with factors such as spatial and temporal variations in climate likely to cause its value to evolve. Despite the existence of numerous forms of the basic law, all preserve this power law dependence of erosion rate on shear stress or a direct equivalent to it, and it is widely recognized that all generally accepted forms of the model can give rise to effectively indistinguishable topographic outputs, given tuning of parameters which cannot be directly measured [e.g., *Tucker and Hancock*, 2010].

[8] Situations where the term $f(q_s, q_c)$ is assumed to be unity can be termed "pure" detachment limited models, and have been deployed extensively in the study of bedrock rivers [*Howard*, 1994] (see also *Whipple* [2004] and *Tucker and Hancock* [2010] for reviews). Importantly, however, real-world tests of the detachment limited model explicitly designed to probe this assumption indicate that this $f(q_s, q_c)$ term is in fact likely to be strongly non-linear, allowing for both promotion and/or inhibition of erosion by sediment flux [*Cowie et al.*, 2008; *Sklar and Dietrich*, 2001; *Turowski and Rickenmann*, 2009; *Valla et al.*, 2010; *Whittaker*, 2007].
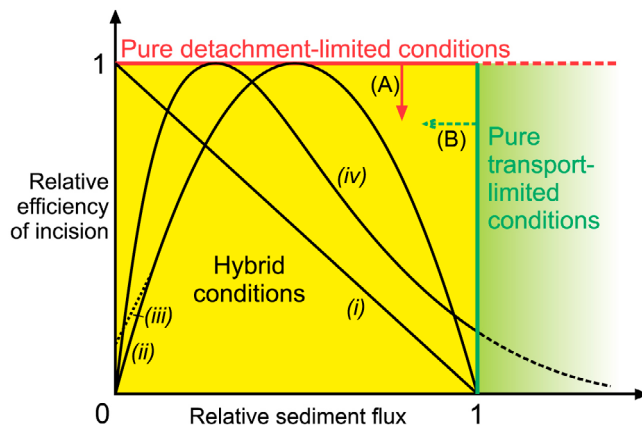
Figure 2. Model space for stream power-based incision laws. Hybrid models shown are (i) linear decline (pure cover) [*Beaumont et al.*, 1992] and three versions of "tools and cover"-type models: (ii) parabolic [*Sklar and Dietrich*, 2004], (iii) almost parabolic [*Gasparini et al.*, 2006], and (iv) *Turowski et al.* [2007] dynamic cover models. All three are based upon detachment limited-type assumptions (i.e., equations (1) and (2)). Note that the pure detachment (red) and transport limited (green) domains are orthogonal. Transport limited conditions are not simply the "end-point" of a pure detachment limited system, and all efficiencies of incision are possible in a sediment-saturated channel (depending on sediment flux divergence downstream, as opposed to its magnitude). Note that values of relative sediment flux greater than 1 are forbidden for incising channels. Small arrows indicate that it is possible to consider the space where incision efficiency is controlled by relative sediment flux (yellow; the main body of the diagram) both from the traditional hybrid detachment limited perspective (A) but also potentially from a modified transport limited perspective (B).

In bedrock rivers, this is because sediment acts as tools to detach bed material, but increasing quantities of bedload sediment in transport will act to cover a greater proportion of the bed, reducing the likelihood of impact against the bed. The ratio of sediment flux, q_s, to carrying capacity of the channel, q_c, appears to control the variation in erosional efficiency [e.g., *Johnson and Whipple*, 2010; *Sklar and Dietrich*, 2004]. This "tools and cover" effect should produce a humped form of $f(q_s, q_c)$ when plotted against q_s/q_c, where the maximum value of $f(q_s, q_c) = 1$ occurs at intermediate values of relative sediment flux within the available range $q_s/q_c = 0$ to 1. However, no actual example of this relation has been well constrained either experimentally or in the field, with authors tending to assume a parabolic or almost parabolic form based on consideration of kinetic energy flux normal to the bed and a static bed cover proportion [*Gasparini et al.*, 2006; *Sklar and Dietrich*, 1998, 2004]. *Turowski et al.* [2007], in contrast, noted that parabolic-type forms do not match laboratory studies of bed abrasion. They showed that allowing for dynamic covering of the bed by sediment and spatial heterogeneity of the armoring of the bed creates an exponential decrease for the cover term. Such an adjustment allowed them to more accurately model the original *Sklar and Dietrich* [2001] experimental results.

[9] The transport limited model (here used synonymously with *Lague*'s [2010] "transport capacity limited model" terminology) in contrast postulates that rates of incision in a channel depend on divergence of sediment carrying capacity, q_c, in the channel, and thus assumes that enough sediment is always available on the channel bed to be incorporated into the flow as required [e.g., *Tucker and Bras*, 1998; *Willgoose et al.*, 1991]. Such models may be written in general form as

$$E = \frac{1}{1 - \lambda_p} \frac{d}{dx} q_c \qquad (3)$$

where λ_p is sediment porosity (which, for simplicity, we shall treat as constant), x is the downstream direction, and q_c is the sediment carrying capacity per unit width in the channel [*Whipple and Tucker*, 2002]. If sediment transport capacity, q_c, in the channel is some function of bed shear stress or a close equivalent, as it is in very many published derivations [see, e.g., *Bagnold*, 1977, 1980; *Einstein*, 1950; *Fernandez Luque and van Beek*, 1976; *Meyer-Peter and Muller*, 1948; *Parker et al.*, 1982; *Schoklitsch*, 1962; *Yalin*, 1963], then we may simply use the chain rule to express the transport limited equation (3) as

$$E = \frac{1}{(1 - \lambda_p)} \left(\frac{dq_c}{d\tau} \cdot \frac{d\tau}{dx} \right). \qquad (4)$$

We can now see the relative effects of variation in each of the primary controlling variables of transport capacity and shear stress separately. This proves useful in distinguishing the erosion models as described in section 2.3.

2.2. Hybrid Erosion Models

[10] Figure 2 shows the position of the pure detachment limited (i.e., equations (1) and (2)) and transport limited (i.e., equations (3) and (4)) erosion laws plotted in terms of sediment flux and efficiency of erosion. The detachment limited model occurs when erosion is not inhibited by sediment cover, and the transport limited condition occurs when the river is not undersupplied with sediment (i.e. it has as much or more sediment than it can transport). The shaded square area bounded by these two erosion models corresponds to systems where interplay of sediment flux and carrying capacity can control erosion rates, which are frequently termed "hybrid" erosional models. Such models can be thought of as representing situations where neither clast transport downstream nor clast detachment from the bed can happen at a rate much faster than the other. Several existing suggested forms of hybrid models are shown within this domain in Figure 2. Note that these all treat the hybrid domain within the detachment limited erosion law as described in section 2.1: the $f(q_s/q_c)$ term in equations (1) and (2) models the effects of the sediment in the channel by modulating a direct function of shear stress on the bed, as opposed to its divergence downstream.

[11] Other authors have also approached the problem of describing sediment flux and capacity dependent river systems without employing the DL-TL framework described here. Such models [e.g., *Beaumont et al.*, 1992; *Braun and Sambridge*, 1997; *Coulthard et al.*, 1999, 2002; *Davy and Lague*, 2009; *Hancock and Anderson*, 2002] treat erosion and deposition in the stream as independent but linked

processes, many using a characteristic travel length for a particle once it is in transit. We acknowledge the potential of such methods to describe these intermediate cases, but do not consider them here. We make this decision partly on the grounds of frequent difficulty in replicating scaling relations (particularly channel concavity) seen in natural systems using such approaches (e.g., *Whipple* [2004], though this issue has now been addressed by *Davy and Lague* [2009]), and partly as such models tend to require parameters (e.g., particle step lengths) which may be challenging to derive for real field data. However, these alternative methods should be seen as complementary to the DL-TL system: the same kinematics can arise from both treatments, and they represent contrasting idealized descriptions of the same underlying real processes. We anticipate that a better understanding of channel response within one framework will lead to better understanding of the mechanics of the other.

2.3. Discrimination Between Models

[12] Authors have tended to use qualitative observations of channel properties to distinguish incision models [e.g., *Anderson*, 1994; *Kirby and Whipple*, 2001; *Snyder et al.*, 2000; *Whittaker et al.*, 2008]. Typically "bedrock" rivers are described as detachment limited systems, as the rock's cohesion is likely to make it harder to detach particles than to transport them. The opposite rationale is often applied to clastic substrates: since the bed is already composed of particles, it is likely to be easier to make them mobile than to transport them. This line of logic may be treacherous; bedrock may be highly fractured, and sediment may still resist mobilization at any given transport stage due to particle-particle interactions. It is important to be able to test explicitly the applicability of each of these models to real river systems.

[13] Previous authors have treated the problem of distinguishing between incision models by discriminating between channel long profile form (and its evolution) resulting from each model type [see, e.g., *Whipple*, 2004; *Attal et al.*, 2011; *Valla et al.*, 2010]. Under equilibrium conditions in which channel erosion is everywhere equal to uplift in the landscape, the pure detachment limited and transport limited erosion laws (and indeed hybrid cases [e.g., *Turowski et al.*, 2007]) give rise to indistinguishable longitudinal channel profiles. However, they lead to fundamentally distinct response styles as landscapes undergo transient response to changes in boundary conditions, such as in climatic or tectonic forcing [e.g., *Whipple and Tucker*, 2002]. This is important, since these transient conditions are those which hold promise for reconstructing past conditions affecting a landscape, and moreover the recent, Plio-Pleistocene sedimentary record may be dominated by sediment export from transiently responding systems [*Zhang et al.*, 2001]. Transient conditions also underpin predictions of landscape response to future climate change. When perturbed by a step displacement at the foot of a channel network, pure detachment limited models of incision where $f(q_s, q_c) = 1$ and where any thresholds are negligible typically lead to a wave-like response that propagates upstream. A sharp break in channel slope demarks a boundary between a downstream reach where the channel is fully adjusted to the new boundary conditions and an upstream reach where the channel remains unaffected. This outcome contrasts with the predictions of

the transport limited end member model wherein all points in the network respond gradually and together to a change in boundary conditions [*Whipple and Tucker*, 2002; *Wobus et al.*, 2006]. Less work has focused on the defining dynamics, response characteristics and long profile forms of hybrid, detachment limited systems where $f(q_s, q_c) \neq 1$. An exception is the work of *Gasparini et al.* [2006, 2007], who have explored the transient dynamics of such a system in which $f(q_s, q_c)$ is allowed to vary, modeling both just the cover effect in isolation (linearly falling $f(q_s, q_c)$ with q_s/q_c) and an almost-parabolic form of the function incorporating both tools and cover. They demonstrated more complex responses combining elements of both diffusive and advective behavior. Similar combined diffusive/advective responses were also shown by *Kooi and Beaumont* [1994] and *Davy and Lague* [2009] using particle step models with variable transport distances analogous to the hybrid models discussed in this work.

[14] However, with access to good quality field data, discrimination between models for an incising channel system need not be based on qualitative assessment of channel form. Rather, it is possible to examine the primary driving parameters (shear stresses, sediment fluxes) and channel response (spatial and temporal variation of incision rate) directly. For a given pattern of shear stress distribution downstream, the two incision rules, equations (2) and (4), predict quite different distributions of channel incision (Figure 3). This is true regardless of the forms of the sediment flux dependent terms $f(q_s, q_c)$ and $dq_c/d\tau$, neither of which is well established across timescales of landscape evolution. In other words, shear stress distribution downstream is a key discriminator for which erosion law is appropriate for a given setting, if its erosion history is known or can be inferred.

[15] We illustrate this idea by a hypothetical example (Figure 3). We consider two possible contrasting channel shear stress distributions (Figures 3a and 3b), then illustrate schematically possible instantaneous incision responses expected under detachment and transport limited models (Figures 3c–3f), including possible sediment flux effects (see Figure 3 caption). The form of each instantaneous incision response shown by the curves in Figures 3c–3f is uniquely associated with the shear stresses producing it (Figures 3a and 3b). This uniqueness is due to the contrast between the power function of shear stress shown in the detachment limited equation (2) and the differential of shear stress shown in the transport limited equation (4). Therefore, locations where either $(\tau - \tau_0) = 0$ or $d\tau/dx = 0$ must record zero incision in the detachment limited and transport limited laws respectively. Varying the sediment flux dependent term ($f(q_s, q_c)$) in the detachment limited law allows for the incision maxima to be translated up or downstream (e.g., solid arrows), but cannot translate these zero points upstream or downstream.

[16] Thus comparison between positions of maxima, minima and zero points in the downstream distributions of incision and shear stress in natural channels forms a key diagnostic tool for differentiating between these two incision models. While Figure 3 presents only an instantaneous channel response under each of these models, as long as the cumulative incision remains relatively small (i.e., little change in long profile form since incision began, and the considered shear stress still reflects its time integrated
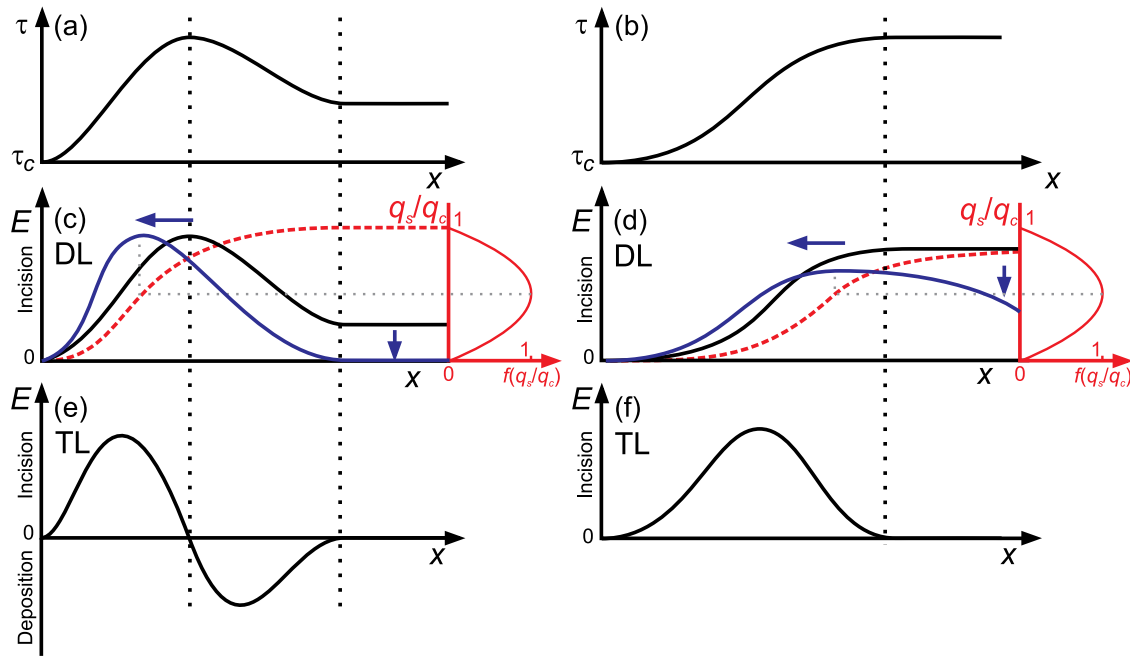
Figure 3. Schematic erosive responses under contrasting erosion models to two hypothetical downstream shear stress distributions. (a, b) Two contrasting hypothetical shear stress distributions which might be seen in a real mountain river channel which is transiently responding to a perturbation. Lower plots show schematically the form of corresponding instantaneous incision patterns under the (c, d) detachment limited (DL) model and the (e, f) transport limited (TL) model. Black curves correspond to the pure DL and TL models, with $f(q_s, q_c) = 1$. These are the simplest possible reference cases. Blue solid curves and associated marker arrows represent the general case for the DL model; the sediment flux dependent term is now a parabolic humped function responding to the relative sediment flux, q_s/q_c, as shown along the right hand axis [e.g., *Sklar and Dietrich*, 2004]. The dashed red curve shows a likely distribution for downstream sediment flux under these conditions, which modulates the pattern of incision. Where the TL model predicts deposition to occur, magnitude is schematic, and assumed to behave simply as "negative incision," i.e., deposition is also governed by equation (4). Location of the start of an aggrading reach remains unaffected by this assumption. Vertical dotted black lines mark positions where $d\tau/dx = 0$.

equivalent), we can reliably use direct comparison between shear stresses and cumulative incision patterns to discriminate between models. In line with other authors [e.g., *Valla et al.*, 2010] we emphasize that the patterns of incision downstream alone are not sufficient to differentiate amongst the models: for example, note the strong similarity between Figures 3c and 3f under different incision laws.

3. Field Data

3.1. Field Area

[17] Our study area is in the Ladakh range of the northwest Indian Himalaya (Figure 4). The site comprises a set of around 70 subparallel catchments cut into the batholith forming the range. These drain from the ridgeline down its southwest flank into the river Indus, which flows northwest along the foot of the massif. The batholith is effectively monolithologic, composed of granodioritic crystalline rocks, but the floors of the valleys are thickly mantled with coarse, loose, very poorly sorted postglacial debris which creates a relatively flat, easily traceable surface (Figure 5) [see also *Hobley et al.*, 2010]. All channel incision is into this material, and never into bedrock. This creates the ambiguity in

choice between incision models: the looseness and small grain size of a large fraction of the substrate suggests a transport limited approach, but a detachment limited approach is also possible due to the immobility of the coarse fraction.

[18] The upper reaches of catchments draining the range divide all show signs of significant carving by flowing ice, with prominent U-shaped valleys and reduced valley gradients compared to the lower reaches (Figures 5 and 6). This has created a knick zone in the long profile of these channels. The extent of this glacial remolding is variable along the batholith, probably driven by variations in the altitude of each catchment [*Jamieson et al.*, 2004]. This glacial alteration of valley form, and particularly development of the knick zone, has perturbed the fluvial network and induced the transient response that we focus on in this work.

[19] The present form of the landscape is best described as three distinct downstream divisions: a domain in the headwaters where the present long profile has changed little from the original postglacial surface, a domain in the middle part of the axial channel where a gorge records incision into the sediment substrate, and a lower domain where fluvial sediment aggrades above the original postglacial surface [*Hobley et al.*, 2010] (Figures 5 and 6). The gorge in the middle reach
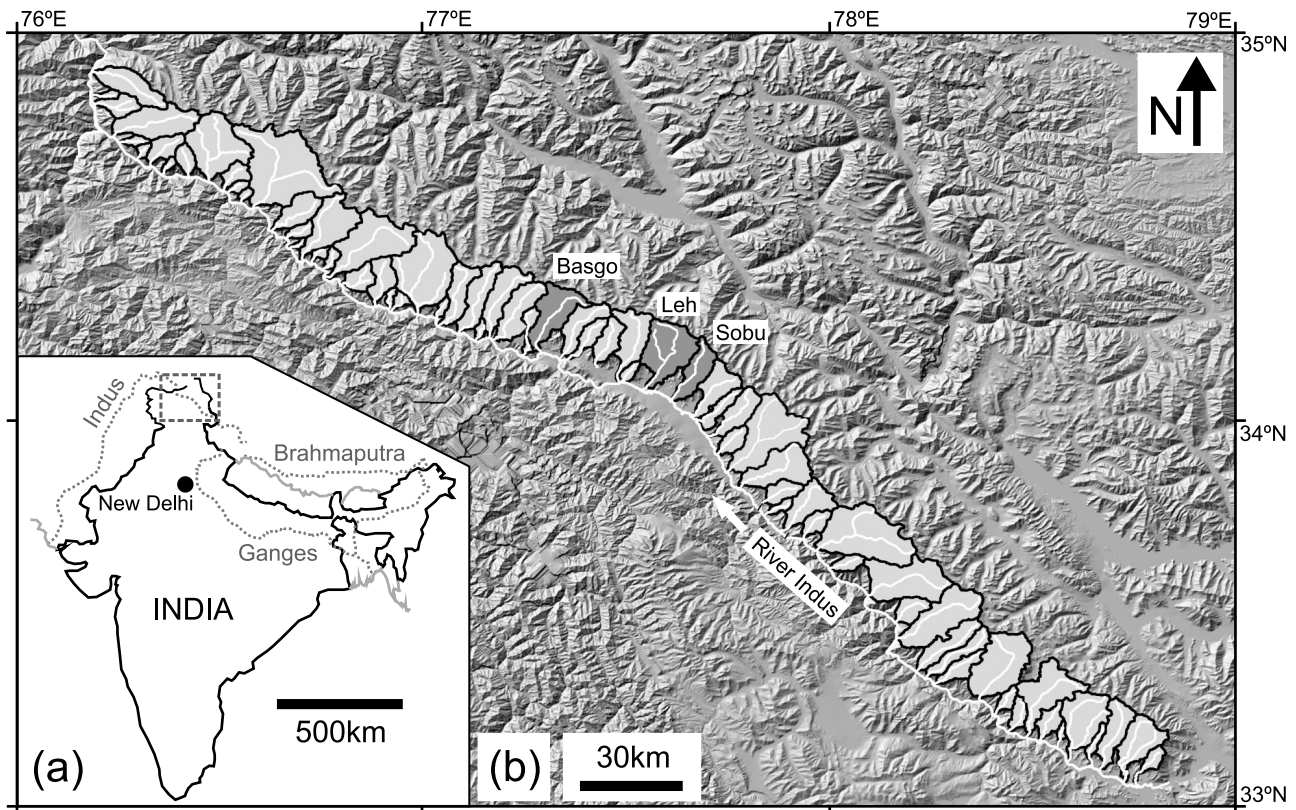
Figure 4. (a) General location map for Ladakh field site. (b) Catchments draining the southeast flank of the Ladakh batholith. Trunk streams are shown in white. The three catchments considered in more detail later in this study, Basgo, Leh and Sobu, are shown in darker gray. The River Indus is shown, and drains northwest along the foot of the batholith (white arrow).

forms the focus of this study, and is decoupled from the bedrock sidewalls of the surrounding glacial trough by the intervening flat, terrace-like surface of the postglacial valley fill. Field evidence also suggests that the lower aggrading domain onlaps this postglacial surface, although the modern channel is slightly inset into the older depositional surface by a couple of meters [*Hobley et al.*, 2010]. These features hint at a somewhat complex movement of this boundary through time, with the aggradational front first advancing up the river system, and then later retreating back down it.

3.2. Data Collection Methodology

[20] We have collected detailed field data in three of the catchments draining the batholith: Basgo, Leh, and Sobu valleys (Figure 4). The dataset incorporates measurements made in all three of the domains described above, but focuses largely on the incised reaches of the middle domain. The data consist of systematic measurements spaced approximately every 300–500 m downstream (where possible) of channel slope on a 30 m scale, current channel depth and width, and the gorge dimensions of depth on either side of the channel and slope of the gorge walls, all measured using a laser range finder. Bankfull depth and width were determined using the height of a sharp boundary between lichen-free and lichen-covered surfaces of boulders in the stream, which was found to be approximately level with the channel banks in the depositional reaches of the channels. To complete the data set we later used remote sensed imagery of the sites freely

available through Google Earth to establish variability of channel and valley floor width downstream in the catchments. In the absence of reliable measurements of channel hydraulic radii, shear stress was then calculated with

$$\tau = \rho_w ghS, \tag{5}$$

where ρ_w is the density of water, g the gravitational acceleration and h the flow depth at bankfull. This equation is appropriate as almost all width/depth ratios exceed 10–20. The reasonableness of these shear stress values was checked by ensuring that the stream discharges calculated from these values using a Darcy-Weisbach friction factor appeared to increase downstream. This approach relies on the assumption that the bankfull discharges are representative of the long term, time-averaged effective eroding discharge.

3.3. Gorge Dimensions and Shear Stress

[21] As described in section 2.3, shear stress data combined with an incision history can discriminate between known incision models. Figure 7 compares gorge depth to channel shear stress distributions downstream for the three channels. The depth of the gorge in the middle reaches shows the expected increase from zero to a maximum, followed by a decrease downstream. However, the data suffer from variations across and down valley introduced by (1) the fact that the pre-incision surface is not perfectly flat, (2) ridges and moraines oriented perpendicular to the valley,

Figure 5. Panoramic view of Leh catchment, looking northwest, taken from Google Earth (© Mapabc.com, Google; images © Cnes/Spot Image, DigitalGlobe). Coloration change in the lower right corner of the image is due to stitching of two images and can be ignored. Field of view is roughly 6 km across. Trunk stream drains southwards (left). The postglacial sediment surface described in the main text is clear, running down from the upper reaches in the U–shaped valley (top right) round the dogleg, through the middle reaches of the valley and disappearing under the broad alluvial depositional domain just after the rock spur which creates a kink in the river planform (lower arrow). Note that this depositional domain now fills the prominent terminal moraine complex in this valley (bottom left corner, downstream of lower arrow). The incised gorge surrounding the trunk stream which we primarily focus on in this work is visible cutting into the postglacial surface in the middle reaches, the start and end of which are marked by the arrows.

and (3) locations where the gorge sidewalls coincide with the rock walls of the glacial trough. To reduce the impact of these variations, we present gorge depth as a five point moving average downstream of the maximum gorge depth present at each site (Figure 7). This also has the advantage of smoothing the data to an appropriate level to stabilize the numerical simulations performed subsequently.

[22] Calculated shear stresses (equation (5)) are plotted alongside gorge depth data (Figure 7) and are also smoothed with a five point moving average to allow direct comparison between the datasets. Figure 7 displays both shear stresses derived for the modern channel and values corrected for the change in bed gradient since incision began. We derive these corrected values by substituting the slope of the incised surface for that of the modern channel in equation (5). In both cases, shear stresses rise from a roughly constant value in the headwaters (only seen in Leh), and return to a roughly constant value around or just before the end of the gorge, but the stable value of shear stress is approximately four times higher downstream of the gorge than the values upstream (see Leh). The peaks are broadly coincident for both the initial and modern values, indicating there has not been a profound change in the distribution through time for the region within the gorge, although for each channel the

modern shear stress maximum is marginally (<1 km) further upstream than its initial position. In all the valleys, maximum shear stresses broadly coincide with maximum gorge depth.

[23] We have also analyzed data describing the gorge sidewall angles, focusing on Basgo and Leh valleys, and discarding any measurements taken where bedrock was known to be exposed in these slopes. These data (N = 54) have a mean of 31.4° and a median of 32.3°, and these values are indistinguishable between valleys. Similarly, analysis of remotely sensed imagery suggests that the width of the valley floor within the gorge does not evolve with distance downstream, and is approximately 40 m in all cases, though with some variation (±10 m) around this value both downstream and between valleys.

[24] In the Leh and Sobu valleys, shear stress becomes almost constant ($d\tau/dx \to 0$) in the modern values approximately 1 km before the end of the modern gorge (Figure 7). This change is less extreme, but still present for Basgo. We infer that this change is related to the onset of aggradation in the channel and associated changes in channel dynamics, and the position of this point is consistent with field evidence that the postglacial surface is onlapped by the fluvial sediments.

3.4. Channel Width and Substrate Grain Size

[25] The distribution of channel widths varies markedly between the three process domains (glacial, incisional and aggradational) outlined above (Figure 8). In the upper glacial domain large variation is present, reflecting changing substrate grain size as the channel passes over and between debris flow fans [cf. *Hobley et al.*, 2010]. In the aggradational domain and within the gorge, channel width is more uniform, with occasional high outliers. Qualitative field observations indicate that localized width maxima within the gorge are sometimes associated with recent localized debris
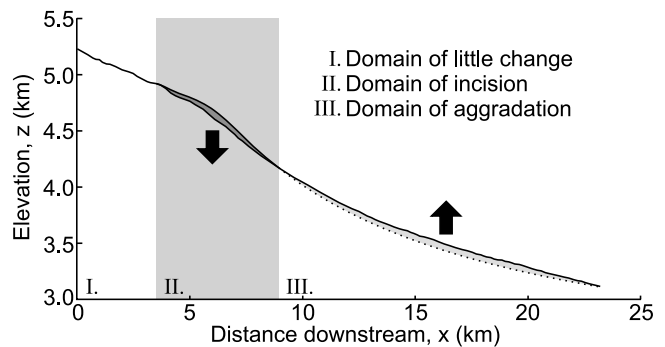
Figure 6. Present long profile form for Leh valley, as example of general form. The three domains are illustrated (Roman numerals), with black arrows indicating sense of motion of the river through time. Dark shading in the middle reaches indicates material removed, and picks out the gorge incised below the postglacial surface. Light shading in the lower reaches indicates material deposited above the original postglacial valley floor (dotted line, shown schematically); likely complexity in the motion of the boundary between these two domains through time is not shown here. Little change through time in the long profile occurs in the upper reaches.

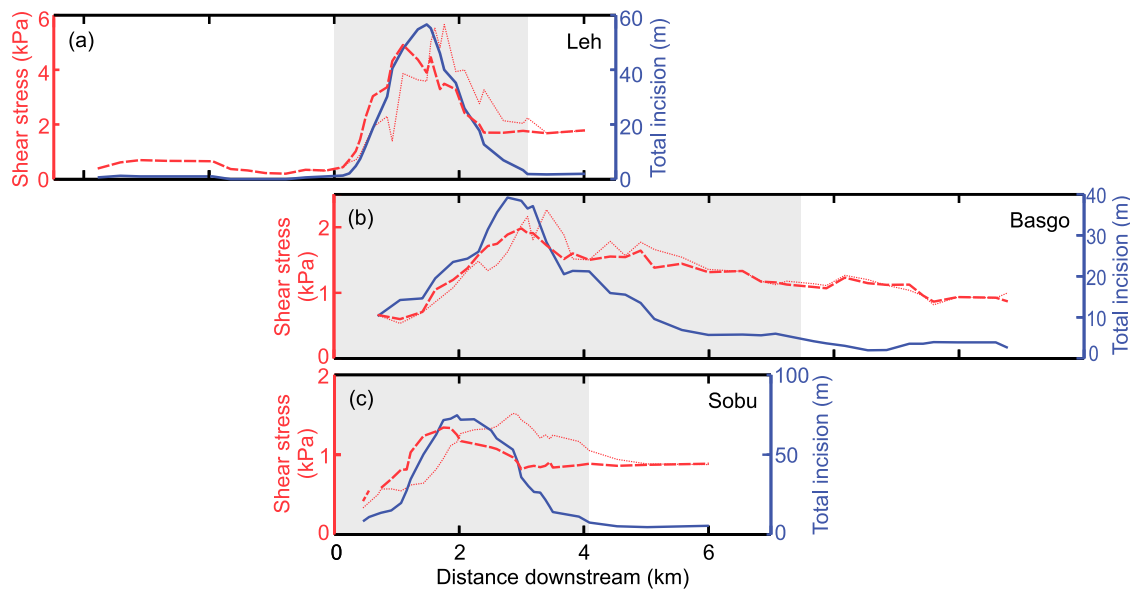**Figure 7.** Downstream distributions for shear stress (red broken lines) and gorge depth (blue solid line) for trunk streams in three catchments: (a) Leh, (b) Basgo, and (c) Sobu. Approximate extent of the gorge is shown by gray shading, and profiles are displayed with the gorge starting points aligned. Heavy red dashed line indicates modern shear stress values in the channel; lighter dotted line plots projected initial shear stress distribution before incision begins, corrected using slope of the incised surface. The distributions are similar, justifying our qualitative comparison of the patterns of these values and the accumulated incision, though note that the shear stress maxima have all migrated upstream through time, again as would be expected in a detachment limited channel but not the transport limited equivalent [*Whipple and Tucker*, 2002]. The maximum gorge depth approximately coincides with these shear stress maxima in each case. Shear stress values at the gorge feet are also often significantly higher than they are at the gorge heads.

flow activity fed from the gorge sidewalls. Importantly, there is only a very weak trend to systematically increasing downstream width in these lower domains, an observation borne out by inspection of the remote sensed imagery.

[26] We have also considered variation in the grain size of the substrate using the Wolman values measured at two different road cut exposures in the Leh valley, approximately 2.5 km apart (see Figure S1 in the auxiliary material).[1] Substrate size distribution is identical between the sites measured (95% confidence; Kolmogorov-Smirnov test), and we assume that this is true of the glacial debris substrate throughout the catchments, consistent with semi-quantitative field observations elsewhere, including field photographs. This observation forms a basis for our treatment of channel aspect ratio variation in the past (section 5.1.5), and demonstrates that the substrate has a uniform resistance to erosion.

4. Channel Response Style

[27] Direct visual comparison of Figures 3 and 7 allows discrimination between detachment and transport limited responses in these catchments. Figure 7 indicates that the maxima in shear stress, and hence the points where $d\tau/dx = 0$, are associated with the maximum gorge depths and not with points of zero incision (compare Figures 3c and 3e). This result is incompatible with the transport limited model

unless shear stress distributions have changed significantly through time, such that the present shear stress distribution does not relate in any way to the time-integrated distribution. We reject this possibility due to the close similarity in form between the modern channel shear stress data and the data corrected to reflect the initial channel slopes as shown in Figure 7. This conclusion is further corroborated by the output of the modeling presented in section 5. We cannot entirely rule out a complex past evolution of shear stress involving significant changes through time, potentially driven by climatically controlled discharge variations. However, such a suggestion is not parsimonious, as it appeals to arbitrary change for which there is no evidence, and which would run counter to the shear stress distributions for which we do have evidence. In such a scenario we might expect to see signs of the implied changes in shear stress preserved in the geomorphology of the gorge floor, for example, as terraces; such signs are absent.

[28] The patterns in Figure 7 are entirely consistent with the detachment limited model (see Figure 3c). We note also that the upstream migration of the shear stress maxima through time in each channel is a result predicted by the detachment limited model, but not by its transport limited equivalent [*Whipple and Tucker*, 2002]. Shear stresses downstream of the gorge are several times greater than those upstream in Leh, but in both of these reaches there is almost no incision. These are the hallmarks of a sediment flux dependent, detachment limited response, as shown schematically in Figure 3c. The raised shear stresses downstream indicate

---

[1]Auxiliary materials are available in the HTML. doi:10.1029/2010JF001935.
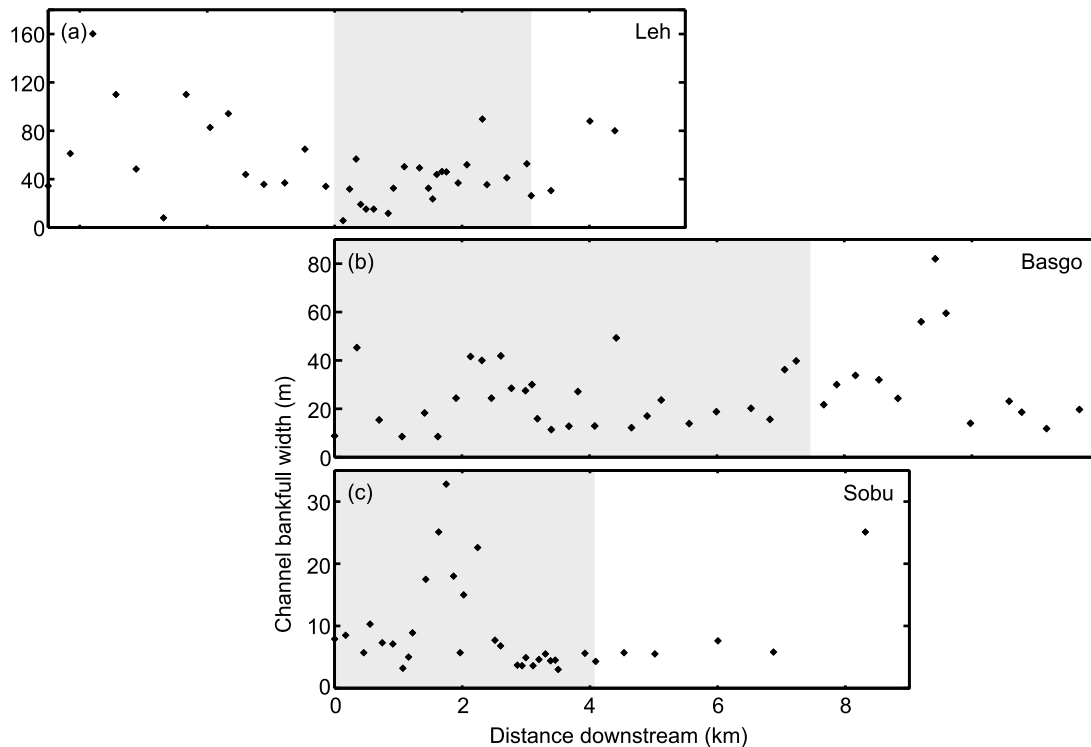
Figure 8. Field measurements of channel bankfull widths for trunk streams, again for the catchments (a) Leh, (b) Basgo, and (c) Sobu. Approximate extent of the gorge is shown by gray shading, and profiles are displayed with the gorge starting points aligned. Measurement error is small compared to the size of the points.

that work is being done in the stream which is not associated with downcutting, and we attribute this to work done moving sediment. In addition, the fact that no incision occurs in the upper domain of Leh valley despite non-zero shear stresses (Figure 7a) demonstrates that this response also involves a shear stress threshold below which no erosion occurs.

[29] To reconstruct sediment flux dependent variation in incision rates, we also need to constrain the magnitude of the sediment flux as it evolves downstream in the gorge. Sediment flux in the channel can be supplied from upstream and from valley sidewalls and floor. There is no evidence for significant amounts of erosion or sediment transport upstream of the gorge. At a coarse scale, this is indicated by the lack of large scale postglacial reshaping of the lower gradient valley floor in this domain; at a finer scale the reach scale fluvial geomorphology involving bouldery fans impinging upon, and deflecting, the main streams also argues against significant sediment mobilization and associated throughput into the gorge below [*Hobley et al.*, 2010]. Within the gorge, hillslopes are at the angle of repose, with a median of 32.3° [cf. *Bagnold*, 1966]. Slopes of loose material at the angle of repose will fail as their base is lowered [*Roering et al.*, 1999; *Strahler*, 1950], and this appears to be the case within the gorge because of the lack of lichen cover on these slopes compared to the hummocky glacial surface [*Hobley et al.*, 2010]. We can therefore calculate sediment flux to the channel by determining the amount of material that must be removed from the hillslope to maintain angle of repose as the channel lowers. In some of the channels, small tributaries also join the main channel within the gorged reaches (see, e.g.,

Figure 5). These will introduce some sediment that our modeling methods (as described below) do not budget for. However, these channels are only strongly incised for a short distance upstream of where they join the main channel, indicating they do not contribute a significant quantity of sediment. The importance of these channels is also further discussed in section 5.1.3.

5. Incision Model

[30] We have now inferred in section 4 that the Ladakh channels we have studied respond in a detachment limited manner, in which incision depends on sediment flux, and shear stress must exceed a threshold if incision is to occur. We discuss the interpretation and consequences of this result in section 6.1, but at this stage we accept this result as given, and work forward on calibrating the form of the implied nonzero sediment flux function in this detachment limited law. The exceptional quality of the preservation of the incision history in this landscape, the consistency of the form across several examples, and the homogeneous gorge hillslopes tightly coupled to the trunk streams make this possible to a greater extent than in any other field study we are aware of. We use a finite difference approach to model the incision occurring under an excess shear stress incision model modulated by a sediment flux function, and vary the inputs to this using a Monte Carlo Markov Chain method. This technique allows us both to establish the most likely form of the sediment flux function for each catchment, and

to rigorously assess the uncertainties associated with these solutions.

5.1. Approach

[31] The finite difference model tracks the progressive incision history at each measurement point in the gorge, and gorge dimensions for each time step are integrated with the incision rates to calculate the sediment flux for each iteration. Because incision rate evolves in time, so does gorge depth as well as shear and Shields stresses.

5.1.1. Initial Model Setup

[32] Model input consists of downstream distances, the smoothed modern and initial channel slopes and gorge depth data already discussed, and flow depth measurements for each locality. We reconstructed the original, pre-incision distribution of channel slopes by assuming the channel originally flowed over a surface with the same slopes as the preserved terrace level. At the gorge head, all data points within the gorge are included, as well as some just upstream of its start where available. However, in the lower gorge reaches we have interpreted the prominent leveling off of the shear stress data in Leh and Sobu valleys c. 1 km up from the gorge end (Figure 7) as indicating the onset of depositional behavior (section 3.3). We do not include data for localities downstream of these transitions, as although the model indicates where the onset of deposition occurs, it does not accurately quantify the magnitude of aggradation on the valley floor. Similarly we do not consider data points in the final kilometer of Basgo valley, which also shows a leveling off around this point, though less distinctly. We acknowledge that this transition point can migrate as the model evolves and the gorge deepens, but our results indicate that this point is in fact quite stable in these catchments (see section 5.2) and we do not need to remove reaches upstream of these chosen transition points. To investigate further, we also ran some model variations where several more data points were removed from the bottom of the gorge, and found this made little difference to the most likely results obtained. Conveniently, the form of the channels also means that no isolated patches nearer the heads of the gorges reach sediment saturation during the model runs, which the model would similarly not be able to account for.

5.1.2. Sediment Flux Function

[33] We model the gorge incision over 100 ka ($\Delta t = 0.5$ years) using an assumed sediment flux function. This short time step was chosen to ensure numerical stability; we do not model sediment flux variability at this timescale [cf. *Lague*, 2010]. A $Kf(q_s/q_c)$ curve forms the main variable input for the model, assigned between $0 \le q_s/q_c \le 1$. The form is given by

$$Kf(q_s/q_c) = \kappa \left(\left(\frac{q_s}{q_c} \right)^{\nu} + c \right) \exp \left(-\phi \frac{q_s}{q_c} \right) \qquad (6)$$

where κ, ν, ϕ and c are all positive constants. This equation is adopted explicitly for its generality; it allows us to fit a wide variety of peaked, smoothly increasing or smoothly decreasing curve shapes, including a broadly symmetrical form as favored by *Sklar and Dietrich* [2004] for bedrock abrasion, as well as optionally allowing a nonzero value of $Kf(q_s/q_c)$ at $q_s/q_c = 0$ as has been suggested in some models [e.g., *Gasparini et al.*, 2006]. The form of the equation is

also analogous to the dependence of erosion on sediment supply proposed by *Turowski et al.* [2007].

5.1.3. Sediment Flux and Capacity

[34] The value of $Kf(q_s/q_c)$ is allocated using q_s produced by mass balance calculations directly within the model from the gorge form and the incision rate, and also a value for q_c determined from a slightly modified version of the Meyer-Peter Muller (MPM) transport equation (see below). The calculation of q_s assumes that no sediment enters the gorge from upstream of its head or from side tributaries but rather that it is sourced entirely from the gorge hillslopes and channel bed. The three catchments presented here were selected specifically to minimize the impact of sediment brought in from side tributaries, and the geomorphology of the upper reaches of the valleys beyond the gorge head also indicates that little sediment is transported significantly downstream in this domain (section 4) [*Hobley et al.*, 2010]. A pilot study for this work using a simpler, analytic method to derive the form of $f(q_s/q_c)$ has also previously shown that the amount of sediment brought in by these side tributaries does not significantly affect the overall shape or properties of the function [*Hobley et al.*, 2009].

[35] The transport capacity, q_c, for these channels is calculated from

$$q_c = 8C \left(\frac{\rho_s - \rho_w}{\rho_w} g D_{char}^3 \right)^{0.5} (\tau^* - \tau_c^*)^{1.5} \qquad (7)$$

where ρ_s is the density of the sediment, 2700 kgm^{-3}, C an empirical constant, D_{char} a characteristic critical grain size for the system, and τ^* and τ_c^* the bed Shields stress and critical Shields stress respectively [*Meyer-Peter and Muller*, 1948]. Note that this formulation gives a volume flux, not mass flux. D_{char} replaces the median diameter of the sediment in the subsurface, which is inappropriate across such a broad range of grain sizes. Instead, it is calculated to give a consistent relationship between the critical shear stress observed in the field and the critical Shields stress which we derive using the Lamb equation [*Lamb et al.*, 2008] (see section 5.1.4).

[36] C is unity in the MPM equation sensu stricto, but here is a free parameter. This adjustment to the basic form is consistent with previous studies of bedload transport [e.g., *Fernandez Luque and van Beek*, 1976]. We calculate its value heuristically for each catchment, adjusting the input value for successful model runs until the sediment capacity matches the sediment flux at the known modern transition points to depositional behavior at the end of the simulation. Several factors working in concert are likely to be responsible for the high magnitudes of C and its strong variation calculated for the different catchments ($C_{Leh} = 400$, $C_{Basgo} = 1350$, $C_{Sobu} = 3337$): (1) our use of D_{char} in place of D_{50}, and the heterogeneous nature of the grain mixture; (2) significantly elevated and variable transport stages seen in and between the channels [e.g., *Fernandez Luque and van Beek*, 1976]; (3) mismatch between the bankfull discharge used in the equation and the true representative discharge; (4) feedbacks between channel slope, erosion thresholds and flood magnitude stochasticity not modeled here [e.g., *Lague et al.*, 2005]. The last of these effects may be dominant in this case, as discussed in section 5.2.

[37] We have chosen to use the MPM relation instead of one of the very many alternative sediment capacity equations since (1) it is of simple form, (2) it makes predictions based on a small set of variables, predictable back through time, and (3) most previous studies of the tools and cover effect have used this formulation. We recognize that we are using the MPM relation under a circumstance it was not derived to explicitly describe, that of a heterogeneous grain mixture. However, we note that most other transport laws which we could have selected [e.g., *Bagnold*, 1977; *Bagnold*, 1980; *Einstein*, 1950; *Fernandez Luque and van Beek*, 1976; *Meyer-Peter and Muller*, 1948; *Parker et al.*, 1982; *Schoklitsch*, 1962; *Yalin*, 1963] rely on a similar form, analogous to excess shear stress raised to a power of 1.5. The multiplier in front of this tends to be only a weak function of variables which we expect may evolve downstream in our channels. Thus we expect a similar downstream form from many of the relations, and since we can reliably infer the absolute value of sediment flux at the point of sediment saturation from our field observations, we can independently calibrate the function magnitude at capacity. This means the choice of specific function is not critical to the outcome of this study.

5.1.4. Thresholds

[38] We require threshold values for both shear stress and Shields' stress for our equations. We use the Lamb equation [*Lamb et al.*, 2008] to derive the critical Shields stress, which makes this value a weak function of slope:

$$\tau_c^* = 0.15 S^{0.25} \tag{8}$$

We derive values for τ_c for our channels based on consideration of past values of shear stress in the channels, but also incorporating this threshold sensitivity to slope, since Shields stress is given by

$$\tau^* = \frac{\tau}{g(\rho_s - \rho_w)D_{char}} \tag{9}$$

We thus calculated the shear stresses that would have been present in the gorge head at the start of its evolution using the calculated initial values of channel slope, correcting for this slope sensitivity, and adjusted the value of D_{char} uniformly for all streams in order to allow incision everywhere within all gorges but forbid it at all points upstream. The critical value of D_{char} was calculated as 0.229 m, which seems feasible based on the known caliber of the bed sediment at the gorge head. In fact, without this slope sensitivity, it is not possible to select a single value to predict τ_c everywhere at once, providing support for our use of equation (8).

5.1.5. Model Output

[39] The model output is determined by a slightly modified version of equation (2), the general detachment limited erosion equation:

$$dZ\left(1 + \frac{2H}{W_V \tan 32°}\right) = Kf(q_s/q_c)(\tau - \tau_c)dt \tag{10}$$

where dZ is the incremental incision across a time step, H is the total accumulated gorge depth, W_V is the gorge floor width, and dt the length of a short time step. This equation solves to give the value of the combined expression $Kf(q_s/q_c)$. Since the standard sediment flux dependent detachment

limited model treats $0 < f(q_s/q_c) < 1$, we can then rescale the solution to give both K, presumed constant within each valley, and $f(q_s/q_c)$ separately. Note that we assume $a = 1$ in equation (2) to derive equation (10): this is the value theoretically associated with erosion proceeding by plucking of clasts from the bed [*Whipple et al.*, 2000] as we hypothesize is appropriate here, and authors using higher values in the incision law tend to be aiming to implicitly incorporate sediment or threshold effects which we treat here explicitly [*Whipple and Tucker*, 2002]. The variable τ evolves as a function of S throughout the run, which assumes constancy of discharge and channel aspect ratio through time, the latter being a reasonable assumption given the uniform grain size distribution in the glacial substrate [*Finnegan et al.*, 2005]. We take $t = 100,000$ years based on the age of the postglacial valley floor [*Owen et al.*, 2006]. This value has a large uncertainty, but as long as the glacier retreat time is the same in each valley, the absolute value is of little importance as fractional error will be subsumed into the erodibility parameter K. The term inside the brackets on the left hand side of the equation reflects the complexity that as we cut down in a v-shaped gorge, for a unit of downwards incision we must also simultaneously mobilize all the material shed into the channel from the angle of repose hillslopes. We treat the addition of this material as instantaneous and assume it is effectively spread evenly across the valley floor. The uniformity of the substrate, demonstrated 32° hillslopes (sections 3.3 and 3.4) and long time scale considered serve to make these assumptions reasonable.

5.1.6. Optimal Solutions

[40] Our goal is to determine the form of equation (6), or in other words to constrain the coefficients κ, ν, ϕ and c. We treat these coefficients as unknown, and determine their values and the uncertainties in their values using a Monte Carlo Markov Chain MCMC) method. Values of the coefficients are changed after each iteration of the MCMC 'chain' and then accepted or rejected using an acceptance criterion (see below). For each iteration the parameter values deviate from the last accepted parameter value, and this deviation is selected from a Gaussian probability distribution that is bounded by minimum and maximum parameter values. Following standard practice, the standard deviation of the Gaussian distribution of each parameter is set so that the acceptance rate of each iteration is ~33% [*Gelman et al.*, 2004]. This process is iterated upon several thousand times in order to constrain the posterior distribution of the model coefficients [e.g., *Berg*, 2004]. The acceptance criterion is based on the Metropolis-Hastings algorithm [*Hastings*, 1970]. The proposed values of the model coefficients are used to drive the finite difference model of channel evolution across the 100,000 year span of gorge development. The model predicts the depth of gorge incision. This model prediction is then compared to the measured gorge to determine the likelihood of the coefficients in equation (6), based on a maximum likelihood estimator (MLE) of the form

$$MLE = \prod_{i=1}^{n} \exp\left[-\frac{\left(H_i^{meas} - H_i^{mod}\right)^2}{2\sigma_H}\right] \tag{11}$$

where n is the number of data points, H is the depth of the gorge, the superscripts *meas* and *mod* indicate measured and
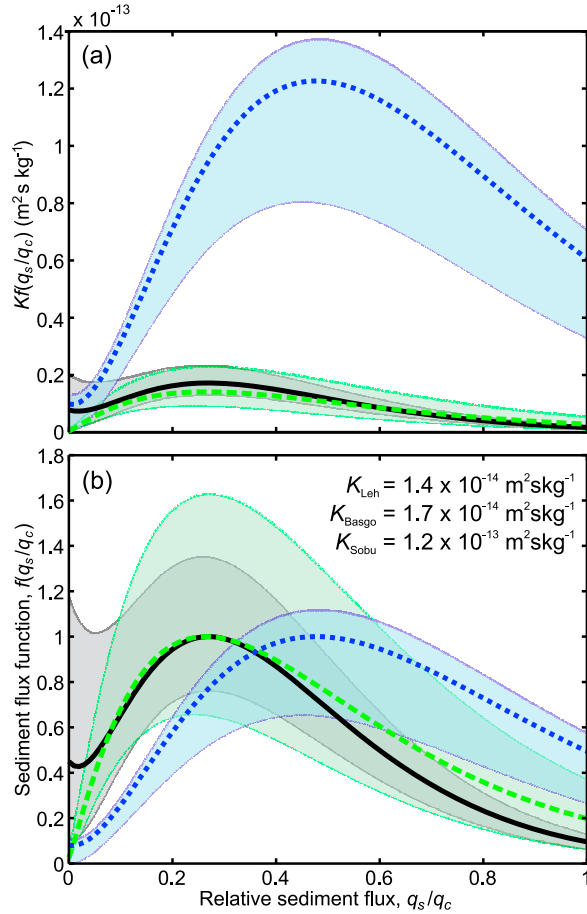
Figure 9. Most likely sediment flux functions for Leh (dashed green line), Basgo (solid black line) and Sobu (dotted blue line) valleys. Shaded areas represent 95% credible intervals for these curves. (a) Comparison of functions preserving best fit magnitude, K. (b) Comparison of functions rescaled to a relative magnitude of 1, consistent with theory. Implied values of K for each catchment are also shown.

modeled values, respectively, and σ_H is an estimate of the variability of the gorge depth, although the value of this has no effect on the outcome of the method (i.e., this value does not change the most likely parameter values or their credibility bounds). The likelihood of the current iteration is compared to the previous iteration. If the ratio likelihood of the new iteration to the previous iteration is >1, then the new coefficient values are accepted. If this ratio is <1, then new coefficients are accepted with a probability equal to the ratio. To generate the posterior distribution of coefficient values, each iteration in the Markov Chain is weighted by the likelihood of the combination of parameter values, creating a probability distribution of each coefficient. This can be used to determine both mean and 95% credibility limits on the parameter values (Figure 9).

5.2. Optimal Results From the Forward Model

[41] Figure 9 shows the most likely forms of the sediment flux function for our channels. We solve for $Kf(q_s/q_c)$ (Figure 9a), and derive the value of K and the form of $f(q_s/q_c)$ by rescaling the latter to give a peak magnitude of unity (Figure 9b). We note that the erosivity, K, of Sobu is much higher than the other two channels (Figure 9a). The associated values of κ, ν, ϕ and c are quoted in Table 1. We plot predicted vs. modeled incision patterns (Figure 10) to illustrate the quality of fit of the sediment flux functions. The matches to the field data are excellent.

[42] We also illustrate the evolution in $f(q_s/q_c)$ values used at each node in the model and resulting changes in incision rates as the best fit runs proceed (Figure 11). Somewhat surprisingly given the freedom of this parameter to evolve, the value of $f(q_s/q_c)$ used by the model, and hence the relative sediment flux itself, is relatively stable at most points downstream. We interpret this to reflect interplay between the evolving gorge cross-sectional form, erosion rates and channel slopes. As the gorge deepens and sediment flux per unit incision increases, erosion rates slow and thus relative fluxes do not strongly vary. In particular the point of maximum erosional efficiency ($f(q_s/q_c) = 1$) moves very little through time, and does not always migrate in the same direction, upstream or downstream (Figure 11). This runs counter to the expected behavior that would be assumed if slope and erosion rates could not evolve during the run, which would predict advance of both the point of maximum erosional efficiency and the transition to aggradational conditions upstream through time. Such stability in the erosional efficiencies through time may account for the difficulties in demonstrating conclusively the existence of sediment flux dependent incision in many other real landscapes.

[43] Note that an advantage of this model is that we have implicitly tested whether a pure detachment limited model would adequately fit this data. Equation (6) will describe a pure detachment limited incision law if both ϕ and ν are equal to 0. Our results show that for all three valleys $\nu \neq 0$, $\phi \neq 0$. The 95% credible interval around each of the three curves as shown in Figure 9 indicates where in each channel's length a pure detachment limited model ($f(q_s/q_c) = 1$) would be statistically indistinguishable from the sediment flux dependent solutions. Our results indicate that the negative feedback between relative sediment flux and incision rates represents a superior fit to a pure detachment limited model at higher sediment fluxes in all channels, and both Leh and Sobu demand a positive feedback at low relative sediment fluxes. We reject the pure detachment limited model as an adequate fit to this data.

[44] We also illustrate the evolving transport stage, the ratio of the Shields stress of the flow to the critical Shields stress, down each channel under these optimal solutions (Figure 12). The different lines shown for each catchment indicate variation in transport stage throughout the model

Table 1. Best Fit Values for Parameters in Equation (10) for Each Channel

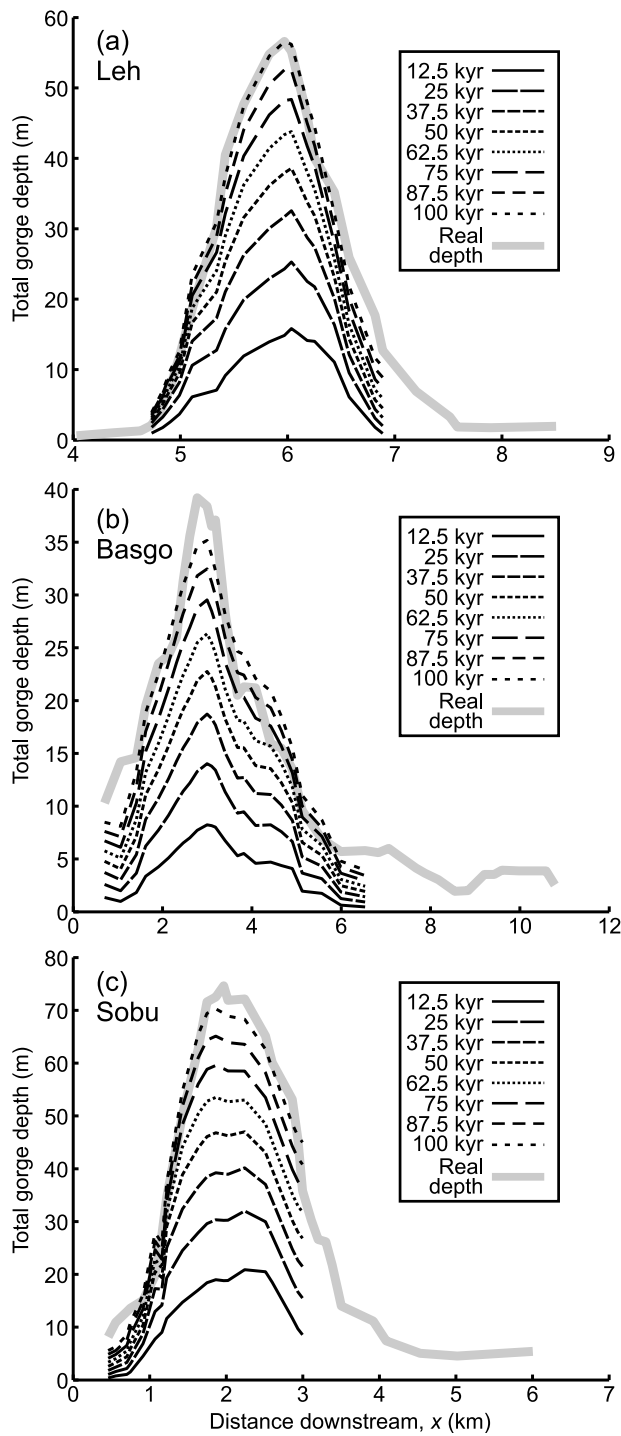| Channel	κ	ν	ϕ	c
Leh	$4.22 \times 10^{-6} < 6.07 \times 10^{-6} < 9.74 \times 10^{-6}$	$1.02 < 1.13 < 1.37$	$7.30 \times 10^{-4} < 1.81 \times 10^{-3} < 4.20 \times 10^{-3}$	$3.64 < 4.24 < 4.89$
Basgo	$2.77 \times 10^{-5} < 3.56 \times 10^{-5} < 4.73 \times 10^{-5}$	$1.69 < 1.91 < 2.05$	$1.81 \times 10^{-3} < 6.83 \times 10^{-3} < 1.76 \times 10^{-2}$	$6.33 < 6.54 < 6.72$
Sobu	$8.76 \times 10^{-5} < 1.26 \times 10^{-4} < 1.39 \times 10^{-4}$	$1.84 < 2.02 < 2.08$	$1.88 \times 10^{-4} < 2.44 \times 10^{-3} < 3.22 \times 10^{-3}$	$3.85 < 4.19 < 4.31$

Figure 10. Outputs from the forward model using most likely solutions shown in Figure 9. Thinner black lines represent the total accumulated incision every eighth of the total runtime, i.e., 12.5 ka. Thicker gray lines are the known field observations of gorge depth. Modeled curves are truncated at the known real transition to depositional behavior in the modern channel.

important since relative stage is also thought to play a role in controlling erosivity in sediment flux dependent incising systems [*Sklar and Dietrich*, 2004; *Whittaker*, 2007], and we go on to discuss its possible effects in sections 6.1 and 6.2. We note that Basgo has slightly higher peak transport stages than Sobu, and Leh has much higher values than both of these. This ordering is consistent with the idea that lower transport stages can be associated with increased
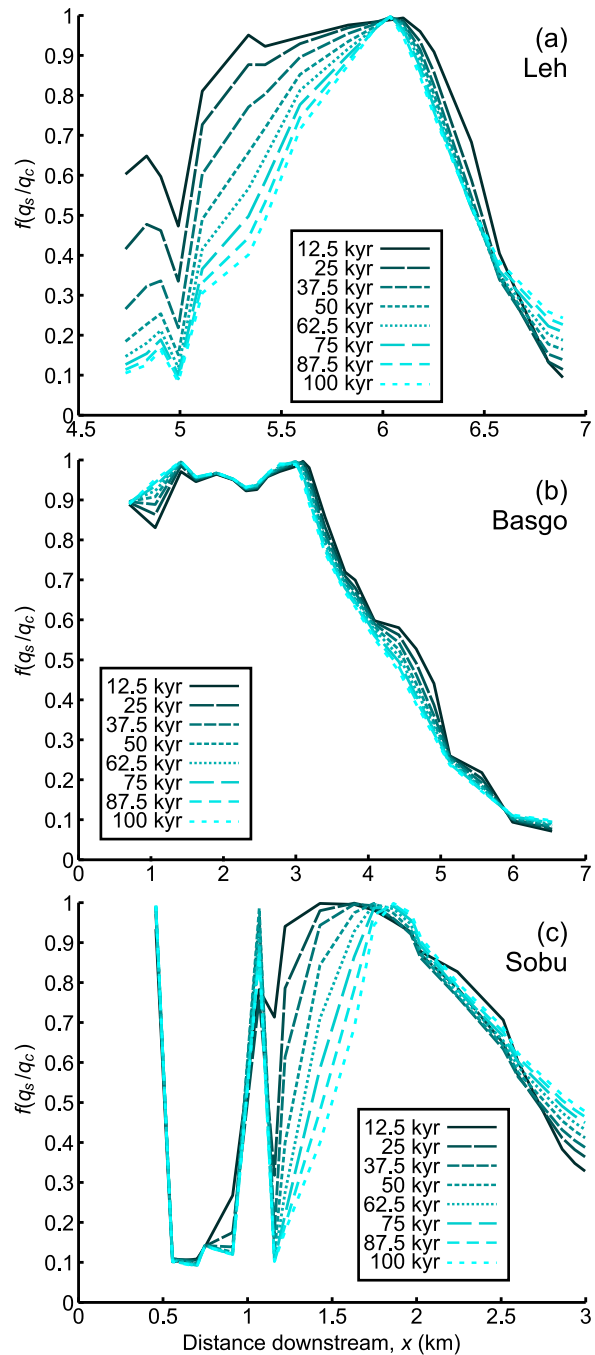

Figure 11. (a–c) Model data reflecting evolution of $f(q_s/q_c)$ at each node downstream during model run for each catchment using most likely solutions (Figure 9). The sharp spike in the Sobu data (Figure 11c) is a point with high error, driven by initially low shear stresses at the gorge head.

runs as slope and sediment load evolve, but overall these values are relatively stable. There is no simple link to the drainage areas of the catchments (A_{Leh} = 123 km^2; A_{Basgo} = 117 km^2; A_{Sobu} = 73 km^2). These transport stages are
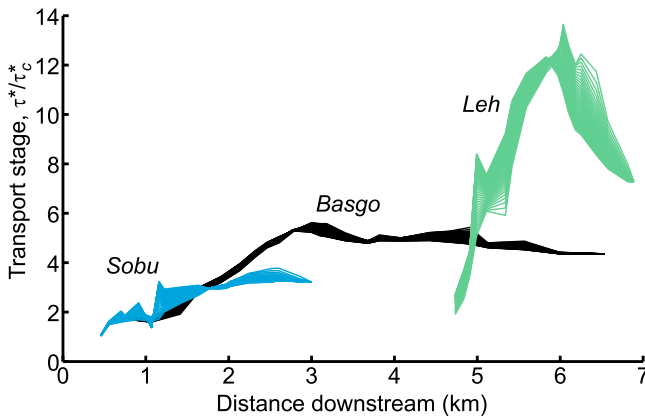
Figure 12. Distributions of transport stage downstream for Leh, Basgo, and Sobu valleys for the most likely sediment flux functions (Figure 9). Each fine line represents transport stage at a single 2.5 ka time-slice during each run; note that although transport stages do evolve during the model runs, they do not vary greatly. The peak transport stages in Leh valley are much (3–5 times) higher than in either Basgo or Sobu valleys, whereas the difference between the Basgo and Sobu distributions is much smaller (< twofold variation).

erosivity, but the large change in erosivity occurs between Basgo and Sobu, while the large change in transport stage occurs between Basgo and Leh.

[45] These transport stages also link to the scaling constants C within the MPM transport law discussed in section 5.1.3. The high transport stages for Leh and low stages for Sobu indicate that Leh will have non-linearly higher effective discharges and hence effective shear stresses than we model here [cf. *Lague et al.*, 2005]. In order for the low transport stage (i.e., threshold dominated) case of Sobu to be comparable with Leh under our approach, its value of C must be disproportionately higher, which it is. Much of the variation in C seen in section 5.1.3 thus probably occurs in order to compensate for this effect under the constant discharge regime we model here.

6. Discussion

6.1. Loose Sediment as a Detachment Limited System

[46] Our field data as presented in Figure 7 and as interpreted in section 4 shows that the river systems discussed in this paper are better described by a detachment limited model, where incision proceeds as a direct function of shear stress, than by a transport limited model, where it proceeds as a function of the divergence of that stress. This is an unexpected and surprising result, since the substrate in this area is composed of loose blocks of material, which a priori might be expected to be transport limited. In physical terms, this indicates that the channels eroding into this material are not able to access enough material from the bed in order to saturate their carrying capacities. In other words, the process of mobilizing the sediment (shear stress dependent) is more difficult than carrying it away (carrying capacity dependent).

[47] The physical mechanism on the channel bed responsible for this outcome is not immediately obvious. Qualitative field observations of the debris have suggest that clast

locking may be an important process during its erosion, as might complex shielding effects where larger grains immobile in essentially all floods limit the potential mobility of smaller grains. This situation is also qualitatively similar to that described by *Topping et al.* [2000] for the Marble and Grand Canyons of the Colorado river. They suggested that the pre-dam, largely sediment-floored Colorado was supply (as opposed to transport) limited with respect to sand and finer clasts on annual timescales due to unavailability of grains of a transportable size on the bed of the river. It is also reminiscent of a scenario described by *Sharmeen and Wilgoose* [2006], whereby an eroding soil can exhibit in part detachment limited behavior as an armor of coarse particles forms over the downwearing surface. In their model, weathering of this armor also produces an element of transport limited behavior in the system; in our case we do not think the clasts in the channel are degrading in an analogous fashion, so this part of their story is likely to be absent here. Nonetheless, similar mechanism for the production of detachment limited behavior in a loose sediment system as in those cases may well apply in this setting: any given flow could transport more sediment than it does, but is unable to saturate as the required additional mass of sediment on the bed is present as clasts larger than the mobility threshold for that flow.

[48] This result is also interesting since it implies that in its long term evolution this clastic river system is behaving more like a bedrock river than an alluvial river. This conclusion is also strengthened by the presence of a "bedrock river-like" form of the $f(q_s/q_c)$ function with both positive ("tools") and negative ("cover") feedbacks present in the data, as discussed further in section 6.2. We note that the term "bedrock river" can itself incorporate a large number of erosion processes, including bed load impact wear, abrasion by suspended load, and plucking [e.g., *Hancock et al.*, 1998; *Whipple et al.* 2000] and can even often be associated with total bed coverage by sediment at various space and time scales. This system is likely to share at least some process elements of these "bedrock" rivers. In light of its detachment limited long term dynamics, we view this erosion process as essentially analogous to plucking in bedrock, where the bed is already divided into discrete units to be mobilized as clasts, but with some nontrivial resistance to the incorporation of these particles into the flow.

[49] As in section 2.2, we again acknowledge that it may be possible to model this erosion of this kind given sufficiently advanced, strictly transport limited mass balance rules. Such a model would likely need to explicitly incorporate a description of the shielding effects of the larger grains on the smaller, flow-dependent thresholds of mobility for each grain size fraction, and variable step lengths for each of these fractions, and/or modeled active layer(s) on the bed [cf. *Chatanantavet and Parker*, 2009; *Coulthard et al.*, 1999, 2002; *Davy and Lague*, 2009; *Hancock and Anderson*, 2002; *Hoey and Ferguson*, 1994; *Lague*, 2010]. The model input would likely also require an *a priori* description of both the grain size distribution of the initial glacial sediment substrate and the stochasticity of the imposed flood history. This approach would have the distinct advantages of allowing us to investigate the physical erosion mechanisms active in this setting in much greater detail, and of fundamentally greater "realism". However, in this field area, and likely in many

others where long term monitoring is not possible, many of the driving variables would be unconstrained in such a model. We have set out with the explicit intention of capturing as much of the system variability as possible with a description of erosion as might be applied in a generic landscape evolution model, rather than to tightly constrain the process mechanics of incision in this area.

6.2. General Form of the Relative Sediment Flux Function

[50] This study has demonstrated that incision proceeding into loose, poorly sorted substrate material across long timescales is well modeled as a detachment limited process, but modulated by a sediment flux function which incorporates both positive and negative feedbacks at different relative sediment fluxes. This pattern has two contrasting physical interpretations, depending on the extent to which we interpret these channels as good analogues to strictly "bedrock" systems. In both cases, the negative feedback is expected *a priori*, but the positive feedback is more unexpected.

[51] 1. These channels are good analogues for bedrock erosion proceeding by plucking [cf. *Chatanantavet and Parker*, 2009]. In this case, we may accurately describe the positive feedback at low relative sediment fluxes as a "tools" effect, and the negative feedback at high relative sediment fluxes as a "cover" effect. The tools effect may then correspond to a reduction of the interparticle locking forces holding the clasts in place by impacting particles, effectively knocking particles out of the bed and into the flow. The cover effect would correspond to a weakening of this effect by shielding of the bed by particles already in transport. The cover effect has been frequently inferred in the field by previous workers [e.g., *Cowie et al.*, 2008; *Johnson et al.*, 2009; *Valla et al.*, 2010], but this study would represent the first well constrained instances of tools effects in single natural river systems. The variable peak position between different channels, its skew towards q_s/q_c < 0.5, and the clearly concave form of the falling limb in at least the Basgo and Leh cases would also provide support for the dynamic bed cover modeling of Turowski and coworkers [e.g., *Turowski et al.*, 2007], and is also compatible with existing experimental studies of the cover effect in an abrading system [*Sklar and Dietrich*, 2001; *Whittaker*, 2007] and with modeling of sediment transport and cover dependent erosion using cellular automata [*Hodge et al.*, 2010].

[52] 2. The channels are best considered exclusively in terms of sediment transport dynamics. In this case it is not strictly accurate to term the positive and negative feedbacks observed in Figure 9 "tools" and "cover" effects, as these terms are only defined for bedrock systems. In such an interpretation, again the appearance of the negative feedback with increasing relative sediment flux is expected, given the Exner equation conserving mass in the channel. However, the positive feedback as seen here has not previously been described in a real sediment floored river. Such a feedback may correspond to a "splash effect" where impacts allow particles to be more readily incorporated into the flow, as previously suggested for aeolian sediment transport [e.g., *Schmeeckle et al.*, 2001]. However, an analogous effect has not previously been recognized in rivers. It is also possible that some complex interaction of multiple variable transport

thresholds between clast size fractions, bed roughness, and/or the imposed discharge stochasticity might account for this positive feedback [e.g., *Venditti et al.*, 2010].

[53] This study leans towards the former interpretation, as we feel that the failure of the transport limited model in describing the erosion occurring makes an interpretation in terms of just transport processes less parsimonious. The key finding here is that the responses of these channels look almost exactly like those we would expect from sediment flux dependent, detachment limited, bedrock systems; we thus prefer an interpretation on this basis. However, as indicated throughout this text, the detachment limited and sediment transport interpretations of this data are at least in part complementary, and not necessarily mutually exclusive.

6.3. The *K* Parameter, Absolute Sediment Flux and the Sobu Curve

[54] Our method has allowed us not only to isolate the form of the sediment flux function, but also the absolute magnitude of the expression $Kf(q_s/q_c)$ for each analyzed channel (Figure 9). The magnitudes of $Kf(q_s/q_c)$ for the Leh and Basgo data sets are significantly lower than that for Sobu, by approximately one order of magnitude. Since the function $f(q_s/q_c)$ varies only between zero and one, this means that the value of K is varying strongly between catchments, with a higher value (more efficient erosion) in Sobu valley. Traditionally, within the stream power law (e.g., equation (1)) the value of K is thought to depend primarily on substrate erodibility, climatic erosivity, and perhaps a threshold effect [e.g., *Whipple*, 2004]. However, Leh and Sobu are adjacent, subparallel valleys, their outlets only some 6 km apart, and are of similar dimensions (Figure 4). Both share the same postglacial substrate within the gorge, and similar elevation spans for each geomorphic domain. It seems unlikely that either the substrate or climate could vary significantly between these valleys.

[55] Our data suggest that some other parameter not captured by the conventional erosion expression must affect the value of K. Studies of the tools and cover effect in flumes as well as theoretical approaches have suggested that this missing expression for this erosion mechanism is transport stage [*Sklar and Dietrich*, 2004; *Whittaker*, 2007]. The transport stage is on average lowest for Sobu (Figure 12), but in order for this effect to be solely responsible for the enhanced erosivity in Sobu valley we would require a very strong decrease in erosivity across a very narrow window in transport stage.

[56] Two effects are more likely to be driving the increased erosivity in Sobu valley.

[57] 1. The interplay of channel slope, incision threshold and discharge stochasticity (as discussed in sections 5.1.3 and 5.2) may mean that the shear stresses produced in the effective discharges for these valleys are not well predicted by our values of τ. As previously noted, Sobu, with its low transport stages (Figure 12), will be subject to this effect more strongly and its high K may in part reflect this.

[58] 2. Absolute sediment flux varies strongly between the valleys, and consistently with the calculated variation in K (Figure 13). The erosivity term within the hybrid detachment limited erosion law in settings similar to this may also be sensitive to absolute bedload flux. Such sensitivity would be consistent with the underlying physics of an
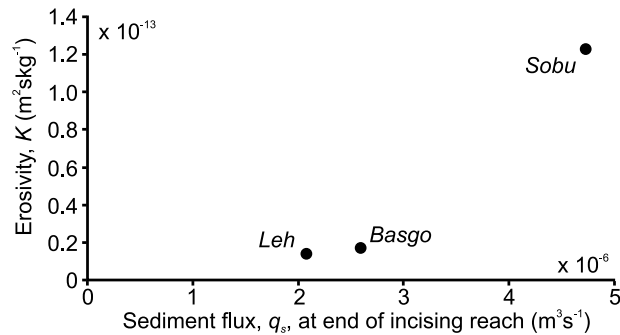
Figure 13. Sediment flux function erosivity, *K*, as a function of modeled total sediment flux at the transition to depositional behavior, measured at the end of model runs using the most likely sediment flux functions (Figure 9).

impact frequency based model for the tools effect, and has previously been incorporated into theoretical models of sediment dependent incision [*Sklar and Dietrich*, 2004; *Turowski et al.*, 2007].

7. Conclusions

[59] We have presented a framework under which the erosion style of an incising channel may be understood as either detachment or transport limited. Shear stress distribution downstream forms the key discriminator between these two erosion models when compared to known patterns of resulting incision in a transiently responding channel network. We have applied this framework in a postglacial landscape where we have calculated shear stress and where incision is well constrained due to the presence of a terrace of known age. We demonstrate for the first time that incision proceeding into a coarse, loose, poorly sorted and partially immobile substrate is best modeled as a sediment flux dependent, detachment limited process. A pure transport limited model is not able to describe this incision. The long term dynamics of the incising reaches of this channel system are more likely to resemble a bedrock rather than an alluvial river.

[60] We demonstrate that the detachment limited erosion law describing these rivers is sediment flux dependent. This sediment dependency incorporates both a negative feedback on erosion rates at high relative sediment fluxes and a positive feedback at low relative sediment fluxes. Uniquely, we are able to calibrate the precise form of the resulting sediment flux function in three different catchments in the field site, and model how transient variations in relative sediment flux control the development of a gorge and the transition to the downstream aggrading system as these catchments develop through time, accurately matching these outcomes to real field data. Specifically, we find that the function is humped and weakly to moderately positively skewed. The falling, negative feedback limb of the function is concave upwards. This form of the function strongly resembles that thought to describe the tools and cover effect in bedrock rivers eroding through impact abrasion by bedload. We also show that the first order erosivity (*K*) of hybrid detachment limited systems is not described sufficiently by extrinsic controls of climate

and lithology, and may also depend on absolute values of sediment flux in the channel.

References

Anderson, R. S. (1994), Evolution of the Santa Cruz Mountains, California, through tectonic growth and geomorphic decay, *J. Geophys. Res.*, *99*(B10), 20,161–20,179, doi:10.1029/94JB00713.

Attal, M., G. E. Tucker, A. C. Whittaker, P. A. Cowie, and G. P. Roberts (2008), Modeling fluvial incision and transient landscape evolution: Influence of dynamic channel adjustment, *J. Geophys. Res.*, *113*, F03013, doi:10.1029/2007JF000893.

Attal, M., P. A. Cowie, A. C. Whittaker, D. Hobley, G. E. Tucker, and G. P. Roberts (2011), Testing fluvial erosion models using the transient response of bedrock rivers to tectonic forcing in the Apennines, Italy, *J. Geophys. Res.*, *116*, F02005, doi:10.1029/2010JF001875.

Bagnold, R. A. (1966), The shearing and dilatation of dry sand and the 'singing' mechanism, *Proc. R. Soc. London, Ser. A*, *295*, 219–232, doi:10.1098/rspa.1966.0236.

Bagnold, R. A. (1977), Bedload transport by natural rivers, *Water Resour. Res.*, *13*(2), 303–312, doi:10.1029/WR013i002p00303.

Bagnold, R. A. (1980), An empirical correlation of bedload transport rates in flumes and natural rivers, *Proc. R. Soc. London, Ser. A*, *372*, 453–473, doi:10.1098/rspa.1980.0122.

Beaumont, C., P. Fullsack, and J. Hamilton (1992), Erosional control of active compressional orogens, in *Thrust Tectonics*, edited by K. R. McClay, pp. 1–18, Chapman and Hall, London.

Berg, B. A. (2004), *Markov Chain Monte Carlo Simulations and Their Statistical Analysis*, World Sci, Singapore.

Braun, J., and M. Sambridge (1997), Modelling landscape evolution on geological time scales: A new method based on irregular spatial discretization, *Basin Res.*, *9*, 27–52, doi:10.1046/j.1365-2117.1997.00030.x.

Burbank, D. W. (2002), Rates of erosion and their implications for exhumation, *Mineral. Mag.*, *66*(1), 25–52, doi:10.1180/0026461026610014.

Chatanantavet, P., and G. Parker (2009), Physically based modeling of bedrock incision by abrasion, plucking and macroabrasion, *J. Geophys. Res.*, *114*, F04018, doi:10.1029/2008JF001044.

Coulthard, T. J., M. J. Kirkby, and M. G. Macklin (1999), Modelling the impacts of Holocene environmental change on the fluvial and hillslope morphology of an upland landscape, using a cellular automaton approach, in *Fluvial Processes and Environmental Change*, edited by A. G. Brown and T. M. Quine, pp. 31–47, John Wiley, Chichester, U. K.

Coulthard, T. J., M. G. Macklin, and M. J. Kirkby (2002), A cellular model of Holocene upland river basin and alluvial fan evolution, *Earth Surf. Processes Landforms*, *27*, 269–288, doi:10.1002/esp.318.

Cowie, P. A., M. Attal, G. E. Tucker, A. C. Whittaker, M. Naylor, A. Ganas, and G. P. Roberts (2006), Investigating the surface process response to fault interaction and linkage using a numerical modelling approach, *Basin Res.*, *18*, 231–266, doi:10.1111/j.1365-2117.2006.00298.x.

Cowie, P. A., A. C. Whittaker, M. Attal, G. P. Roberts, G. E. Tucker, and A. Ganas (2008), New constraints on sediment-flux dependent river incision: Implications for extracting tectonic signals from river profiles, *Geology*, *36*, 535–538, doi:10.1130/G24681A.1.

Davy, P., and D. Lague (2009), Fluvial erosion/transport equation of landscape evolution models revisited, *J. Geophys. Res.*, *114*, F03007, doi:10.1029/2008JF001146.

Einstein, H. A. (1950), The bed-load function for sediment transportation in open channel flows, *Tech. Bull. 1026*, 73 pp., U.S. Dep. of Agric., Washington, D. C.

Fernandez Luque, R., and R. van Beek (1976), Erosion and transport of bed-load sediment, *J. Hydraul. Res.*, *14*, 127–144, doi:10.1080/00221687609499677.

Finnegan, N. J., G. H. Roe, D. R. Montgomery, and B. Hallet (2005), Controls on the channel width of rivers: Implications for modeling fluvial incision of bedrock, *Geology*, *33*, 229–232, doi:10.1130/G21171.1.

Gasparini, N. M., R. L. Bras, and K. X. Whipple (2006), Numerical modeling of non–teady-state river profile evolution using a sediment-

flux-dependent incision model, in *Tectonics, Climate, and Landscape Evolution*, edited by S. D. Willett et al., *Spec. Pap. Geol. Soc. Am.*, *398*, 127–141, doi:10.1130/2006.2398(08).

Gasparini, N. M., K. X. Whipple, and R. L. Bras (2007), Predictions of steady state and transient landscape morphology using sediment-flux-dependent river incision models, *J. Geophys. Res.*, *112*, F03S09, doi:10.1029/2006JF000567.

Gelman, A., J. B. Carlin, H. S. Stern, D. B. Rubin, and D. B. Dunson (2004), *Bayesian Data Analysis*, 2nd ed., Chapman and Hall, London.

Gilbert, G. K. (1877), *Report on the Geology of the Henry Mountains*, Dep. of the Inter., Gov. Print. Off., Washington, D. C.

Hancock, G. S., and R. S. Anderson (2002), Numerical modeling of fluvial strath-terrace formation in response to oscillating climate, *Geol. Soc. Am. Bull.*, *114*(9), 1131–1142.

Hancock, G. S., R. S. Anderson, and K. X. Whipple (1998), Beyond power: Bedrock river incision process and form, in *Rivers Over Rock: Fluvial Processes in Bedrock Channels*, *Geophys. Monogr. Ser*, vol. 107, edited by K. J. Tinkler and E. E. Wohl, pp. 35–60, AGU, Washington, D. C.

Hastings, W. K. (1970), Monte Carlo sampling methods using Markov Chains and their applications, *Biometrika*, *57*(1), 97–109, doi:10.1093/biomet/57.1.97.

Hobley, D. E. J., H. D. Sinclair, and P. A. Cowie (2009), How should we model incision into coarse, loose, heterogeneous grain mixtures in mountain catchments?, *Eos Trans. AGU*, *90*(52), Fall Meet. Suppl., Abstract EP53E-02.

Hobley, D. E. J., H. D. Sinclair, and P. A. Cowie (2010), Processes, rates and time scales of fluvial response in an ancient post-glacial landscape of the northwest Indian Himalaya, *Geol. Soc. Am. Bull.*, *122*, 1569–1584, doi:10.1130/B30048.1.

Hodge, R. A., T. B. Hoey, and L. S. Sklar (2010), A theoretical model of grain mobility in bedrock rivers, paper presented at William Smith Meeting: Landscapes into Rock, Geol. Soc. of London, London.

Hoey, T. B., and R. Ferguson (1994), Numerical simulation of downstream fining by selective transport in gravel bed rivers: Model development and illustration, *Water Resour. Res.*, *30*(7), 2251–2260, doi:10.1029/94WR00556.

Howard, A. D. (1994), A detachment-limited model of drainage basin evolution, *Water Resour. Res.*, *30*(7), 2261–2285, doi:10.1029/94WR00757.

Howard, A. D., and G. Kerby (1983), Channel changes in badlands, *Geol. Soc. Am. Bull.*, *94*, 739–752, doi:10.1130/0016-7606(1983)94<739:CCIB>2.0.CO;2.

Jamieson, S. S. R., H. D. Sinclair, L. A. Kirstein, and R. S. Purves (2004), Tectonic forcing of longitudinal valleys in the Himalaya: Morphological analysis of the Ladakh Batholith, North India, *Geomorphology*, *58*(1–4), 49–65, doi:10.1016/S0169-555X(03)00185-5.

Johnson, J. P. L., and K. X. Whipple (2010), Evaluating the controls of shear stress, sediment supply, alluvial cover and channel morphology on experimental bedrock incision rate, *J. Geophys. Res.*, *115*, F02018, doi:10.1029/2009JF001335.

Johnson, J. P. L., K. X. Whipple, L. S. Sklar, and T. C. Hanks (2009), Transport slopes, sediment cover, and bedrock channel incision in the Henry Mountains, Utah, *J. Geophys. Res.*, *114*, F02014, doi:10.1029/2007JF000862.

Kirby, E., and K. X. Whipple (2001), Quantifying differential rock-uplift rates via stream profile analysis, *Geology*, *29*(5), 415–418, doi:10.1130/0091-7613(2001)029<0415:QDRURV>2.0.CO;2.

Kooi, H., and C. Beaumont (1994), Escarpment evolution on high-elevation rifted margins: Insights derived from a surface processes model that combines diffusion, advection and reaction, *J. Geophys. Res.*, *99*(B6), 12,191–12,209, doi:10.1029/94JB00047.

Lague, D. (2010), Reduction of long-term bedrock incision efficiency by short-term alluvial cover intermittency, *J. Geophys. Res.*, *115*, F02011, doi:10.1029/2008JF001210.

Lague, D., N. Hovius, and P. Davy (2005), Discharge, discharge variability, and the bedrock channel profile, *J. Geophys. Res.*, *110*, F04006, doi:10.1029/2004JF000259.

Lamb, M. P., W. E. Dietrich, and J. G. Venditti (2008), Is the critical Shields stress for incipient sediment motion dependent on channel-bed slope?, *J. Geophys. Res.*, *113*, F02008, doi:10.1029/2007JF000831.

Loget, N., P. Davy, and J. Van Den Driessche (2006), Mesoscale fluvial erosion parameters deduced from modeling the Mediterranean sea level drop during the Messinian (late Miocene), *J. Geophys. Res.*, *111*, F03005, doi:10.1029/2005JF000387.

Meyer-Peter, E., and R. Muller (1948), Formulas for bedload transport, in *Proceedings of the 2nd Meeting of the International Association for Hydraulic Structures Research*, pp. 39–64, Int. Assoc. for Hydraul. Res., Delft, Netherlands.

Milliman, J. D., and J. P. M. Syvitski (1992), Geomorphic/tectonic control of sediment transport to the ocean: The importance of small mountainous rivers, *J. Geol.*, *100*, 525–544, doi:10.1086/629606.

Molnar, P., and P. England (1990), Late Cenozoic uplift of mountain ranges and global climate change: Chicken or egg?, *Nature*, *346*, 29–34, doi:10.1038/346029a0.

Owen, L. A., M. W. Caffee, K. R. Bovard, R. C. Finkel, and M. C. Sharma (2006), Terrestrial cosmogenic nuclide surface exposure dating of the oldest glacial successions in the Himalayan orogen: Ladakh Range, northern India, *Geol. Soc. Am. Bull.*, *118*, 383–392, doi:10.1130/B25750.1.

Paola, C., and V. R. Voller (2005), A generalized Exner equation for sediment mass balance, *J. Geophys. Res.*, *110*, F04014, doi:10.1029/2004JF000274.

Parker, G., P. C. Klingeman, and D. G. McLean (1982), Bedload and size distribution in paved gravel-bed streams, *J. Hydraul. Div. Am. Soc. Civ. Eng.*, *108*, 544–571.

Rodríguez-Iturbe, I., A. Rinaldo, R. Rigon, R. L. Bras, A. Marani, and E. Ijjász-Vásquez (1992), Energy dissipation, runoff production, and the three-dimensional structure of river basins, *Water Resour. Res.*, *28*(4), 1095–1103, doi:10.1029/91WR03034.

Roering, J. J., J. W. Kirchner, and W. E. Dietrich (1999), Evidence for nonlinear, diffusive sediment transport on hillslopes and implications for landscape morphology, *Water Resour. Res.*, *35*(3), 853–870, doi:10.1029/1998WR900090.

Schmeeckle, M. W., J. M. Nelson, J. Pitlick, and J. P. Bennett (2001), Inter-particle collision of natural sediment grains in water, *Water Resour. Res.*, *37*(9), 2377–2391, doi:10.1029/2001WR000531.

Schoklitsch, A. (1962), *Handbuch des Wasserbaues*, 3rd ed., Springer, Vienna.

Sharmeen, S., and G. R. Wilgoose (2006), The interaction between armouring and particle weathering for eroding landscapes, *Earth Surf. Process. Landf.*, *31*(10), 1195–1210, doi:10.1002/esp.1397.

Sklar, L. S., and W. E. Dietrich (1998), River Longitudinal Profiles and Bedrock Incision Models: Strem Power and the Influence of Sediment Supply, in *Rivers Over Rock: Fluvial Processes in Bedrock Channels*, *Geophys. Monogr. Ser*, vol. 107, edited by K. J. Tinkler and E. E. Wohl, pp. 237–260, AGU, Washington, D. C.

Sklar, L. S., and W. E. Dietrich (2001), Sediment and rock strength controls on river incision into bedrock, *Geology*, *29*, 1087–1090, doi:10.1130/0091-7613(2001)029<1087:SARSCO>2.0.CO;2.

Sklar, L. S., and W. E. Dietrich (2004), A mechanistic model for river incision into bedrock by saltating bed load, *Water Resour. Res.*, *40*, W06301, doi:10.1029/2003WR002496.

Snyder, N. P., K. X. Whipple, G. E. Tucker, and D. J. Merritts (2000), Landscape response to tectonic forcing: Digital elevation model analysis of stream profiles in the Mendocino triple junction region, northern California, *Geol. Soc. Am. Bull.*, *112*(8), 1250–1263, doi:10.1130/0016-7606(2000)112<1250:LRTTFD>2.0.CO;2.

Stock, J. D., and D. R. Montgomery (1999), Geologic constraints on bedrock river incision using the stream power law, *J. Geophys. Res.*, *104*(B3), 4983–4993, doi:10.1029/98JB02139.

Strahler, A. N. (1950), Equilibrium theory of erosional slopes approached by frequency distribution analysis, *Am. J. Sci.*, *248*, 673–696, doi:10.2475/ajs.248.10.673.

Topping, D. J., D. M. Rubin, and L. E. Vierra Jr. (2000), Colorado River sediment transport 1. Natural sediment supply limitation and the influence of Glen Canyon Dam, *Water Resour. Res.*, *36*(2), 515–542, doi:10.1029/1999WR900285.

Tucker, G. E., and R. L. Bras (1998), Hillslope processes, drainage density, and landscape morphology, *Water Resour. Res.*, *34*(10), 2751–2764, doi:10.1029/98WR01474.

Tucker, G. E., and G. S. Hancock (2010), Modelling landscape evolution, *Earth Surf. Processes Landforms*, *35*, 28–50, doi:10.1002/esp.1952.

Turowski, J. M., and D. Rickenmann (2009), Tools and cover effects in bedload transport observations in the Pitzbach, Austria, *Earth Surf. Processes Landforms*, *34*, 26–37, doi:10.1002/esp.1686.

Turowski, J. M., D. Lague, and N. Hovius (2007), Cover effect in bedrock abrasion: A new derivation and its implications for the modeling of bedrock channel morphology, *J. Geophys. Res.*, *112*, F04006, doi:10.1029/2006JF000697.

Valla, P. G., P. A. van der Beek, and D. Lague (2010), Fluvial incision into bedrock: Insights from morphometric analysis and numerical modeling of gorges incising glacial hanging valleys (western Alps, France), *J. Geophys. Res.*, *115*, F02010, doi:10.1029/2008JF001079.

van der Beek, P. A., and P. Bishop (2003), Cenozoic river profile development in the Upper Lachlan catchment (SE Australia) as a test of quantitative fluvial incision models, *J. Geophys. Res.*, *108*(B6), 2309, doi:10.1029/2002JB002125.

Venditti, J. G., W. E. Dietrich, P. A. Nelson, M. A. Wydzga, J. Fadde, and L. S. Sklar (2010), Effect of sediment pulse grain size on sediment transport rates and bed mobility in gravel bed rivers, *J. Geophys. Res.*, *115*, F03039, doi:10.1029/2009JF001418.

Whipple, K. X. (2004), Bedrock rivers and the geomorphology of active orogens, *Annu. Rev. Earth Planet. Sci.*, *32*(1), 151–185, doi:10.1146/annurev.earth.32.101802.120356.

Whipple, K. X., and G. E. Tucker (1999), Dynamics of the stream-power river incision model: Implications for height limits of mountain ranges, landscape response timescales and research needs, *J. Geophys. Res.*, *104*(B8), 17,661–17,674, doi:10.1029/1999JB900120.

Whipple, K. X., and G. E. Tucker (2002), Implications of sediment-flux-dependent river incision models for landscape evolution, *J. Geophys. Res.*, *107*(B2), 2039, doi:10.1029/2000JB000044.

Whipple, K. X., G. S. Hancock, and R. S. Anderson (2000), River incision into bedrock: Mechanics and relative efficacy of plucking, abrasion, and cavitation, *Geol. Soc. Am. Bull.*, *112*(3), 490–503, doi:10.1130/0016-7606(2000)112<490:RIIBMA>2.0.CO;2.

Whittaker, A. C. (2007), Investigating controls on bedrock river incision using natural and laboratory experiments, Ph.D. thesis, 188 pp, Univ. of Edinburgh, Edinburgh, U. K.

Whittaker, A. C., M. Attal, P. A. Cowie, G. E. Tucker, and G. P. Roberts (2008), Decoding temporal and spatial patterns of fault uplift using transient river long profiles, *Geomorphology*, *100*, 506–526, doi:10.1016/j.geomorph.2008.01.018.

Willett, S. D., and M. T. Brandon (2002), On steady states in mountain belts, *Geology*, *30*, 175–178, doi:10.1130/0091-7613(2002)030<0175:OSSIMB>2.0.CO;2.

Willgoose, G., R. L. Bras, and I. Rodriguez-Iturbe (1991), A coupled channel network growth and hillslope evolution model: 1. Theory, *Water Resour. Res.*, *27*(7), 1671–1684, doi:10.1029/91WR00935.

Wobus, C. W., B. T. Crosby, and K. X. Whipple (2006), Hanging valleys in fluvial systems: Controls on occurrence and implications for landscape evolution, *J. Geophys. Res.*, *111*, F02017, doi:10.1029/2005JF000406.

Yalin, M. S. (1963), An expression for bed bed-load transportation, *J. Hydraul. Div. Am. Soc. Civ. Eng.*, *89*(3), 221–250.

Zeitler, P. K., et al. (2001), Erosion, Himalayan geodynamics, and the geomorphology of metamorphism, *GSA Today*, *11*(1), 4–9, doi:10.1130/1052-5173(2001)011<0004:EHGATG>2.0.CO;2.

Zhang, P., P. Molnar, and W. R. Downs (2001), Increased sedimentation rates and grain sizes 2–4 Myr ago due to the influence of climate change on erosion rates, *Nature*, *410*, 891–897, doi:10.1038/35073504.

P. A. Cowie, Department of Earth Science, University of Bergen, PO Box 7803, Bergen N-5020, Norway.

D. E. J. Hobley, Department of Environmental Sciences, University of Virginia, Clark Hall, 291 McCormick Rd., Charlottesville, VA 22904, USA. (dan.hobley@virginia.edu)

S. M. Mudd and H. D. Sinclair, School of GeoSciences, University of Edinburgh, Drummond Street, Edinburgh EH8 9XP, UK.